Dispersion in Anisotropic Media Modeled by Three-Dimensional TLM

Christian Huber, Michael Krumpholz, *Member, IEEE*, and Peter Russer, *Fellow, IEEE*

Abstract—**The dispersion in anisotropic media modeled by three-dimensional TLM is investigated. Two nodes, the symmetrical condensed node with stubs and the symmetrical super-condensed node are considered. Simple closed-form expressions for the dispersion relations do not exist in general, therefore the investigations are restricted to wave propagation in isotropic media and to wave propagation along the mesh axes and the mesh diagonals. The dispersion analysis for the symmetrical super-condensed node yields a direct relationship between the relative permittivity and relative permeability and the parameters of the scattering matrix.**

I. Introduction

FOR the modeling of distributed circuits with arbitrary geometries including also anisotropic media, numerical methods based on the discretization of Maxwell's equations like the finite difference time domain (FDTD) method [1] or the transmission line matrix (TLM) method [2] have become more and more popular due to their high flexibility. For the three-dimensional TLM modeling of anisotropic media, various TLM schemes based on different nodes have been developed and tested successfully [2]–[5]. However, there have been only a few investigations about the dispersion of these three-dimensional TLM schemes. Some results on the dispersion in a mesh of expanded TLM nodes with stubs, of symmetrical condensed nodes (SCN) with stubs and of symmetrical super-condensed nodes (SSCN) have been given [6]–[8]. Considering the dispersion relations is important since deviations from the linear dispersion behavior degrade the accuracy of the field computation. Furthermore, from the dispersion relations, unphysical modes, i.e., modes not converging to solutions of Maxwell's equations may be identified. In this paper, a systematic comparison of the dispersion behavior and of the occurrence of unphysical modes is given for the SCN with stubs and for the SSCN.

The dispersion relations for wave propagation in free space have already been calculated in the literature for various FDTD and TLM schemes [9]–[13]. We use a general approach for the computation of the dispersion relations based on the state space representation of the discretized electromagnetic field [14]–[16]. The dispersion relations of the two investigated TLM schemes are calculated from the solutions of the eigenvalue problem in the field state space. We distinguish between physical and unphysical eigenvectors in the field state space. Physical eigenvectors describe solutions of the TLM scheme which converge to solutions of Maxwell's equations for frequencies or discretization intervals approaching zero, whereas unphysical eigenvectors describe spurious solutions which are introduced by the discretization of Maxwell's equations [17].

The paper is organized in three parts. In the first part, the plane wave solutions of Maxwell's equations are investigated. The approach is similar to the approach presented in [18]. In general, there are no simple closed-form expressions for the dispersion relations of Maxwell's equations describing wave propagation in anisotropic media. Therefore, we restrict our further investigations to the cases in which simple expressions for the dispersion relations of Maxwell's equations exist. These cases are the wave propagation in isotropic media and the wave propagation along the mesh axes and mesh diagonals in symmetric anisotropic media. In the second and third part, for these cases, we investigate the dispersion of the TLM schemes for the SCN with stubs and for the SSCN. A simple closed-form expression for the dispersion relation exists for the SSCN modeling isotropic media [8]. For all other investigated cases, the polynomials representing the implicit dispersion relations are given. Approximating the polynomials of the SSCN for wave propagation along the mesh axes yields a direct relationship between the parameters of the scattering matrix and the relative permittivity and relative permeability in symmetric anisotropic media.

II. Plane Wave Solutions of Maxwell's Equations

Maxwell's equations for anisotropic media are given by

$$\nabla \times \mathbf{H} = \boldsymbol{\varepsilon} \frac{\partial \mathbf{E}}{\partial t} \tag{1}$$

$$\nabla \times \mathbf{E} = -\boldsymbol{\mu} \frac{\partial \mathbf{H}}{\partial t}. \tag{2}$$

In the principal coordinate system, the permittivity tensor $\boldsymbol{\varepsilon}$ and the permeability tensor $\boldsymbol{\mu}$ for symmetric media are given by

$$\boldsymbol{\varepsilon} = \begin{bmatrix} \varepsilon_x & 0 & 0 \\ 0 & \varepsilon_y & 0 \\ 0 & 0 & \varepsilon_z \end{bmatrix}$$

and

Manuscript received October 3, 1994; revised April 24, 1995. This work was supported by the Deutsche Forschungsgemeinschaft.

C. Huber is with the Ferdinand-Braun-Institut für Höchstfrequenztechnik, 12489 Berlin, Germany.

M. Krumpholz was at the Ferdinand-Braun-Institut für Höchstfrequenztechnik. He is now with the Radiation Laboratory, EECS Department of the University of Michigan, Ann Arbor, MI 48109-2122 USA.

P. Russer is with the Ferdinand-Braun-Institut für Höchstfrequenztechnik and with the Lehrstuhl für Hochfrequenztechnik, Technische Universität München, 80333 München, Germany.

IEEE Log Number 9412680.

$$\boldsymbol{\mu} = \begin{bmatrix} \mu_x & 0 & 0 \\ 0 & \mu_y & 0 \\ 0 & 0 & \mu_z \end{bmatrix}. \tag{3}$$

In cartesian components, Maxwell's equations may be written as

$$\begin{bmatrix} \varepsilon_x \frac{\partial}{\partial t} & 0 & 0 & 0 & -\frac{\partial}{\partial z} & \frac{\partial}{\partial y} \\ 0 & \varepsilon_y \frac{\partial}{\partial t} & 0 & \frac{\partial}{\partial z} & 0 & -\frac{\partial}{\partial x} \\ 0 & 0 & \varepsilon_z \frac{\partial}{\partial t} & -\frac{\partial}{\partial y} & \frac{\partial}{\partial x} & 0 \\ 0 & -\frac{\partial}{\partial z} & \frac{\partial}{\partial y} & -\mu_x \frac{\partial}{\partial t} & 0 & 0 \\ \frac{\partial}{\partial z} & 0 & -\frac{\partial}{\partial x} & 0 & -\mu_y \frac{\partial}{\partial t} & 0 \\ -\frac{\partial}{\partial y} & \frac{\partial}{\partial x} & 0 & 0 & 0 & -\mu_z \frac{\partial}{\partial t} \end{bmatrix} \cdot \begin{bmatrix} E_x \\ E_y \\ E_z \\ H_x \\ H_y \\ H_z \end{bmatrix} = 0. \tag{4}$$

From (4), we obtain in spectral domain

$$\boldsymbol{M}[E_x, E_y, E_z, H_x, H_y, H_z]^T = 0 \tag{5}$$

where we have introduced the matrix

$$\boldsymbol{M} = \begin{bmatrix} \omega\varepsilon_x & 0 & 0 & 0 & k_z & k_y \\ 0 & \omega\varepsilon_y & 0 & k_z & 0 & k_x \\ 0 & 0 & \omega\varepsilon_z & k_y & k_x & 0 \\ 0 & k_z & k_y & -\omega\mu_x & 0 & 0 \\ k_z & 0 & k_x & 0 & -\omega\mu_y & 0 \\ k_y & k_x & 0 & 0 & 0 & -\omega\mu_z \end{bmatrix}. \tag{6}$$

The cartesian components of the wavevector $\vec{k}$ are k_x, k_y, and k_z. The angular frequency ω is related to the frequency f by $\omega = 2\pi f$. For any nontrivial solution (5) requires [18]

$$\det(\boldsymbol{M}) = 0 \tag{7}$$

which yields a characteristic polynomial in ω, k_x, k_y, and k_z

$$\omega^2(C_2\omega^4 - C_1\omega^2 + C_0) = 0 \tag{8}$$

with

$$\begin{aligned} C_2 &= \varepsilon_x\varepsilon_y\varepsilon_z\mu_x\mu_y\mu_z \\ C_1 &= k_x^2(\varepsilon_r\varepsilon_z\mu_x\mu_y + \varepsilon_x\varepsilon_y\mu_x\mu_z) \\ &\quad + k_y^2(\varepsilon_x\varepsilon_y\mu_y\mu_z + \varepsilon_y\varepsilon_z\mu_x\mu_y) \\ &\quad + k_z^2(\varepsilon_x\varepsilon_z\mu_y\mu_z + \varepsilon_y\varepsilon_z\mu_x\mu_z) \\ C_0 &= k_x^2k_y^2(\varepsilon_x\mu_y + \varepsilon_y\mu_x) + k_x^2k_z^2(\varepsilon_x\mu_z + \varepsilon_z\mu_x) \\ &\quad + k_y^2k_z^2(\varepsilon_y\mu_z + \varepsilon_z\mu_y) + k_x^4\varepsilon_x\mu_x \\ &\quad + k_y^4\varepsilon_y\mu_y + k_z^4\varepsilon_z\mu_z. \end{aligned} \tag{9}$$

Equation (8) has six solutions ω_i representing the dispersion relations of the six possible plane wave solutions for Maxwell's equations in symmetric anisotropic media. The solution $\omega_{1,2} = 0$ represents a stationary solution corresponding to the electro- and magnetostatic case. The other four solutions $\omega_{3,4,5,6}$ correspond to propagating plane wave solutions of Maxwell's equations. In general, simple closed-form expressions do not exist for $\omega_{3,4,5,6}$ [18]. In case of wave propagation along the x-axis and in (1, 0, 0) direction, respectively, we have $k_y = k_z = 0$ and obtain from (8)

$$\omega^2(k_x^2 - \varepsilon_y\mu_z\omega^2)(k_x^2 - \varepsilon_z\mu_y\omega^2) = 0. \tag{10}$$

Similar expressions may be derived for wave propagation along the y- and z-axis. For wave propagation along the diagonal in the x–y-plane and in (1, 1, 0) direction, respectively, we have $k_x = k_y$ as well as $k_z = 0$ yielding

$$\omega^2\left[(\varepsilon_x + \varepsilon_y)k_x^2 - \varepsilon_x\varepsilon_y\mu_z\omega^2\right] \cdot \left[(\mu_x + \mu_y)k_x^2 - \varepsilon_z\mu_x\mu_y\omega^2\right] = 0. \tag{11}$$

Similar expressions may be derived for wave propagation along the diagonals in the x–z- and y–z-plane. A significant simplification of (8) is also given for isotropic media leading to

$$\omega^2(k_x^2 + k_y^2 + k_z^2 - \varepsilon\mu\omega^2)^2 = 0. \tag{12}$$

Of course, analyzing the dispersion of a TLM scheme, we can only expect to find simple algebraic expressions for the cases in which simple algebraic expressions exist for Maxwell's equations. Therefore, for the dispersion analysis of the TLM method with stub-loaded SCN and SSCN, we will restrict ourselves to the three cases described by (10), (11), and (12).

III. THE DISPERSION ANALYSIS OF TLM WITH STUB-LOADED SCN

Using the state space representation for the electromagnetic field presented in [14]–[16], the amplitudes of all incident and scattered waves are summarized in the Hilbert space vectors

$$|a\rangle = \sum_{k,l,m,n=-\infty}^{+\infty} {}_k\boldsymbol{a}_{l,m,n}|k; l, m, n\rangle$$

and

$$|b\rangle = \sum_{k,l,m,n=-\infty}^{+\infty} {}_k\boldsymbol{b}_{l,m,n}|k; l, m, n\rangle. \tag{13}$$

The complete electromagnetic field state is represented by a single vector $|a\rangle$ and $|b\rangle$, respectively, in the field state space $\mathcal{H}_W$. The field state space is a product space of three vectors spaces, $\mathcal{H}_W = \mathcal{C}^r \otimes \mathcal{H}_m \otimes \mathcal{H}_t$. In the r-dimensional complex vector space $\mathcal{C}^r$, all the r wave amplitudes of the TLM node with the coordinates k, l, m, and n are summarized in the vectors ${}_k\boldsymbol{a}_{l,m,n}$ and ${}_k\boldsymbol{b}_{l,m,n}$, respectively. The indices l, m, n, and k are the discrete space and time indices related to the space and time coordinates via $x = l\Delta l$, $y = m\Delta l$, $z = n\Delta l$ and $t = k\Delta t$ where Δl and Δt represent the space and time discretization interval. To each mesh node with the coordinates l, m, and n, we assign a base vector $|l, m, n\rangle$. The set of vectors $|l, m, n\rangle$ is an orthonormal base of the Hilbert space $\mathcal{H}_m$. The time states are represented by the base vectors $|k\rangle$ in the Hilbert space $\mathcal{H}_t$. The base vectors $|k;\, l,\, m,\, n\rangle = |k\rangle \otimes |l,\, m,\, n\rangle$ fulfill the orthogonality relations

$$\langle k_1;\, l_1,\, m_1,\, n_1 | k_2;\, l_2,\, m_2,\, n_2\rangle = \delta_{k_1,\,k_2}\delta_{l_1,\,l_2}\delta_{m_1,\,m_2}\delta_{n_1,\,n_2}. \tag{14}$$

In TLM the instantaneous propagation of all wave pulses in the mesh between adjacent node ports may be described by

$$|a\rangle = \boldsymbol{\Gamma}|b\rangle. \tag{15}$$

The connection operator $\boldsymbol{\Gamma}$ relates the waves scattered by the TLM cells with the waves incident into the neighboring TLM cells. In the TLM Hilbert space representation, $\boldsymbol{\Gamma}$ is a matrix of space shift operators [14]. The equation

$$|b\rangle = \boldsymbol{TS}|a\rangle \tag{16}$$

describes the simultaneous scattering at all the mesh nodes. $\boldsymbol{S}$ is the scattering matrix of the TLM node and $\boldsymbol{T}$ is the time shift operator defined by

$$\boldsymbol{T}|k;\, l,\, m,\, n\rangle = |k+1;\, l,\, m,\, n\rangle \tag{17}$$

thus indicating that the scattering by a mesh node is connected with the time delay Δt. Eliminating the scattered wave amplitudes, we obtain the eigenvalue equation

$$(\boldsymbol{\Gamma TS} - 1)|a\rangle = 0 \tag{18}$$

in the field state space $\mathcal{H}_W$. We introduce new base vectors of $\mathcal{H}_t$,

$$|\Omega\rangle = \sum_{k=-\infty}^{+\infty} e^{jk\Omega}|k\rangle_t \tag{19}$$

with the normalized frequency $\Omega = 2\pi\Delta t f$, as well as new base vectors for $\mathcal{H}_m$,

$$|\chi,\, \eta,\, \xi\rangle = \sum_{l,\,m,\,n=-\infty}^{+\infty} e^{j(\chi l + \eta m + \xi n)}|l,\, m,\, n\rangle \tag{20}$$

with the normalized wave vector components $\chi = \Delta l k_x$, $\eta = \Delta l k_y$, and $\xi = \Delta l k_z$. As shown in [13], restricting the dispersion analysis to the case of plane wave propagation, (18) yields

$$\left(\overline{\boldsymbol{\Gamma}}\boldsymbol{S} - e^{j\Omega}\right)\vec{a}(\chi,\, \eta,\, \xi) = 0 \tag{21}$$

in frequency and wave vector domain. The vector of the plane wave amplitudes, $\vec{a}(\chi,\, \eta,\, \xi)$, is given by

$$\vec{a}(\chi,\, \eta,\, \xi) = \sum_{l,\,m,\,n=-\infty}^{+\infty} {}_k\boldsymbol{a}_{l,\,m,\,n} e^{-j(\chi l + \eta m + \xi n)}. \tag{22}$$

The connection operator in wave vector domain, $\overline{\boldsymbol{\Gamma}}$, represents an r-dimensional matrix with the elements $e^{j\chi}$, $e^{j\eta}$, and $e^{j\xi}$. (21) requires

$$\det\left(\overline{\boldsymbol{\Gamma}}\boldsymbol{S} - e^{j\Omega}\right) = 0 \tag{23}$$

for any nontrivial eigenvector $\vec{a}(\chi,\, \eta,\, \xi)$.

The scattering of the wave amplitudes at one stub-loaded SCN is described by a 18×18 matrix [3]. In comparison with the SCN for the free space [3], six stubs have been added in order to model dielectric and magnetic media. The scattering matrix in symmetrical notation [16], [19] is given by

$$\boldsymbol{S} = \begin{bmatrix} \boldsymbol{S}_0 & \boldsymbol{K}^T \\ \boldsymbol{K} & \boldsymbol{L} \end{bmatrix} \tag{24}$$

where

$$\boldsymbol{S}_0 = \begin{bmatrix} \boldsymbol{\alpha}_1 & \boldsymbol{\beta}_1 & \boldsymbol{\beta}_2 \\ \boldsymbol{\beta}_1^T & \boldsymbol{\alpha}_2 & \boldsymbol{\beta}_3 \\ \boldsymbol{\beta}_2^T & \boldsymbol{\beta}_3^T & \boldsymbol{\alpha}_3 \end{bmatrix} \tag{25}$$

with

$$\begin{aligned}
\boldsymbol{\alpha}_1 &= \begin{bmatrix} a_{yz} & c_{yz} & 0 & 0 \\ c_{yz} & a_{yz} & 0 & 0 \\ 0 & 0 & a_{zy} & c_{zy} \\ 0 & 0 & c_{zy} & a_{zy} \end{bmatrix} \\
\boldsymbol{\alpha}_2 &= \begin{bmatrix} a_{zx} & c_{zx} & 0 & 0 \\ c_{zx} & a_{zx} & 0 & 0 \\ 0 & 0 & a_{xz} & c_{xz} \\ 0 & 0 & c_{xz} & a_{xz} \end{bmatrix} \\
\boldsymbol{\alpha}_3 &= \begin{bmatrix} a_{xy} & c_{xy} & 0 & 0 \\ c_{xy} & a_{xy} & 0 & 0 \\ 0 & 0 & a_{yx} & c_{yx} \\ 0 & 0 & c_{yx} & a_{yx} \end{bmatrix} \\
\boldsymbol{\beta}_1 &= \begin{bmatrix} 0 & 0 & d_z & -d_z \\ 0 & 0 & -d_z & d_z \\ b_z & b_z & 0 & 0 \\ b_z & b_z & 0 & 0 \end{bmatrix} \\
\boldsymbol{\beta}_2 &= \begin{bmatrix} 0 & 0 & b_y & b_y \\ 0 & 0 & b_y & b_y \\ d_y & -d_y & 0 & 0 \\ -d_y & d_y & 0 & 0 \end{bmatrix} \\
\boldsymbol{\beta}_3 &= \begin{bmatrix} 0 & 0 & d_x & -d_x \\ 0 & 0 & -d_x & d_x \\ b_x & b_x & 0 & 0 \\ b_x & b_x & 0 & 0 \end{bmatrix}
\end{aligned} \tag{26}$$

as well as (27), shown at the bottom of the next page, and

$$\boldsymbol{L} = \begin{bmatrix} g_x & 0 & 0 & 0 & 0 & 0 \\ 0 & g_y & 0 & 0 & 0 & 0 \\ 0 & 0 & g_z & 0 & 0 & 0 \\ 0 & 0 & 0 & h_x & 0 & 0 \\ 0 & 0 & 0 & 0 & h_y & 0 \\ 0 & 0 & 0 & 0 & 0 & h_z \end{bmatrix}. \tag{28}$$

The matrix elements for the subscripts $i,\, j \in \{x;\, y;\, z\}$ are given by

$$\begin{aligned}
a_{i,\,j} &= -\frac{Y_i}{2(Y_i+4)} + \frac{Z_j}{2(Z_j+4)} \\
b_i &= \frac{2}{Y_i+4} \\
c_{i,\,j} &= -\frac{Y_i}{2(Y_i+4)} - \frac{Z_j}{2(Z_j+4)} \\
d_i &= \frac{2}{Z_i+4} \\
e_i &= \frac{2\sqrt{Y_i}}{Y_i+4}
\end{aligned}$$

$$\begin{aligned} f_i &= \frac{2\sqrt{Z_i}}{Z_i + 4} \\ g_i &= \frac{Y_i - 4}{Y_i + 4} \\ h_i &= -\frac{Z_i - 4}{Z_i + 4} \end{aligned} \tag{29}$$

wherein

$$\begin{aligned} Z_x &= 4\left(\mu_{rx}\frac{\Delta y \Delta z}{\Delta x \Delta l} - 1\right) \\ Z_y &= 4\left(\mu_{ry}\frac{\Delta x \Delta z}{\Delta y \Delta l} - 1\right) \\ Z_z &= 4\left(\mu_{rz}\frac{\Delta x \Delta y}{\Delta z \Delta l} - 1\right) \\ Y_x &= 4\left(\varepsilon_{rx}\frac{\Delta y \Delta z}{\Delta x \Delta l} - 1\right) \\ Y_y &= 4\left(\varepsilon_{ry}\frac{\Delta x \Delta z}{\Delta y \Delta l} - 1\right) \\ Y_z &= 4\left(\varepsilon_{rz}\frac{\Delta x \Delta y}{\Delta z \Delta l} - 1\right) \end{aligned} \tag{30}$$

with $\mu_{ri} = \mu_i/\mu_0$ and $\varepsilon_{ri} = \varepsilon_i/\varepsilon_0$. For the dispersion analysis of the SCN with stubs, we assume $\Delta x = \Delta y = \Delta z = \Delta l$. In this case, the connection operator in wave vector domain is given by

$$\begin{aligned} \boldsymbol{\Gamma} = & e^{-j\chi}(\boldsymbol{\Delta}_{1,2} + \boldsymbol{\Delta}_{3,4}) + e^{j\chi}(\boldsymbol{\Delta}_{2,1} + \boldsymbol{\Delta}_{4,3}) \\ & + e^{-j\eta}(\boldsymbol{\Delta}_{5,6} + \boldsymbol{\Delta}_{7,8}) + e^{j\eta}(\boldsymbol{\Delta}_{6,5} + \boldsymbol{\Delta}_{8,7}) \\ & + e^{-j\xi}(\boldsymbol{\Delta}_{9,10} + \boldsymbol{\Delta}_{11,12}) + e^{j\xi}(\boldsymbol{\Delta}_{10,9} + \boldsymbol{\Delta}_{12,11}) \quad (31) \\ & + \boldsymbol{\Delta}_{13,13} + \boldsymbol{\Delta}_{14,14} + \boldsymbol{\Delta}_{15,15} - \boldsymbol{\Delta}_{16,16} \\ & - \boldsymbol{\Delta}_{17,17} - \boldsymbol{\Delta}_{18,18} \end{aligned} \tag{32}$$

with the 12 × 12 (m, n)-matrix $(\boldsymbol{\Delta}_{m',n'})_{m,n} = \delta_{m',m}\delta_{n',n}$.

We consider wave propagation in (1, 0, 0) direction in symmetric anisotropic media. In this case, we have $\eta = \xi = 0$. There are eighteen eigenvalues $\lambda_i = e^{j\Omega_i}$ of (21) and eighteen solutions of the characteristic (23), respectively. Ten of the eigenvalues are given by

$$\lambda_{1,2} = 1$$

and

$$\lambda_{3,\cdots,10} = -1. \tag{33}$$

The eigenvectors corresponding to these eigenvalues describe nonpropagating solutions in a TLM mesh. As $\lambda = 1$ implies $\Omega = 0$, the eigenvalues $\lambda_{1,2}$ represent the electro- and magnetostatic case. As $\lambda = -1$ implies $\Omega = \pi$, the eigenvectors corresponding to $\lambda_{3,\ldots,10}$ are unphysical eigenvectors oscillating with the frequency $f = 1/(2\Delta t)$. The other eight eigenvalues are given implicitly by the following factors of the characteristic equation

$$C_{0i}\lambda^4 + C_{1i}\lambda^3 + 2C_{2i}\lambda^2 + C_{1i}\lambda + C_{0i} = 0 \tag{34}$$

and with $\lambda = e^{j\Omega}$ by

$$C_{0i}\cos(2\Omega) + C_{1i}\cos(\Omega) + C_{2i} = 0. \tag{35}$$

The two factors of the characteristic equation are specified by the two different sets of coefficients

$$\begin{aligned} C_{01} &= (4 + Y_y)(4 + Z_z) \\ C_{11} &= 2(2Y_y + 2Z_z + Y_yZ_z)[\cos(\chi) - 1] \\ C_{21} &= Y_yZ_z - 2(8 + 2Y_y + 2Z_z + Y_yZ_z)\cos(\chi) \end{aligned} \tag{36}$$

and

$$\begin{aligned} C_{02} &= (4 + Y_z)(4 + Z_y) \\ C_{12} &= 2(2Y_z + 2Z_y + Y_zZ_y)[\cos(\chi) - 1] \\ C_{22} &= Y_zZ_y - 2(8 + 2Y_z + 2Z_y + Y_zZ_y)\cos(\chi). \end{aligned} \tag{37}$$

We approximate (35) for frequencies and wave numbers approaching zero using $\cos x \approx 1 - x^2/2$ and obtain

$$\left[4k_x^2 - (4 + Y_y)(4 + Z_z)\frac{\Delta t^2}{\Delta l^2}\omega^2\right] \cdot \left[4k_x^2 - (4 + Y_z)(4 + Z_y)\frac{\Delta t^2}{\Delta l^2}\omega^2\right] = 0 \tag{38}$$

and

$$\left[k_x^2 - 4\varepsilon_{ry}\mu_{rz}\frac{\Delta t^2}{\Delta l^2}\omega^2\right] \cdot \left[k_x^2 - 4\varepsilon_{rz}\mu_{ry}\frac{\Delta t^2}{\Delta l^2}\omega^2\right] = 0 \tag{39}$$

respectively. With the well-known relation $c_0/c_m = 1/2$ [3], where c_0 represents the wave propagation velocity of the free space and $c_m = \Delta l/\Delta t$ the velocity of the wave pulses in the TLM mesh, (39) is identical with the dispersion relation of the propagating plane wave solutions of Maxwell's equations given by (10). For wave propagation along the y- and z-axis, a dispersion analysis yields similar results.

Fig. 1 illustrates the dispersion in a TLM mesh for wave propagation in (1, 0, 0) direction in a symmetric anisotropic medium with $\varepsilon_{rx} = 8$, $\varepsilon_{ry} = 2$, $\varepsilon_{rz} = 1.5$ and $\mu_{rx} = 2$, $\mu_{ry} = 1$, $\mu_{rz} = 2.5$. For the figures in this paper, we generally consider only the eigenvalues describing propagating solutions of the TLM scheme. In the diagram, there are two branches of the linear dispersion curve corresponding to the solutions

$$\boldsymbol{K} = \begin{bmatrix} 0 & 0 & 0 & 0 & 0 & 0 & e_x & e_x & e_x & e_x & 0 & 0 \\ e_y & e_y & 0 & 0 & 0 & 0 & 0 & 0 & 0 & 0 & e_y & e_y \\ 0 & 0 & e_z & e_z & e_z & e_z & 0 & 0 & 0 & 0 & 0 & 0 \\ 0 & 0 & 0 & 0 & -f_x & f_x & 0 & 0 & 0 & 0 & f_x & -f_x \\ 0 & 0 & f_y & -f_y & 0 & 0 & 0 & 0 & -f_y & f_y & 0 & 0 \\ -f_z & f_z & 0 & 0 & 0 & 0 & f_z & -f_z & 0 & 0 & 0 & 0 \end{bmatrix} \tag{27}$$

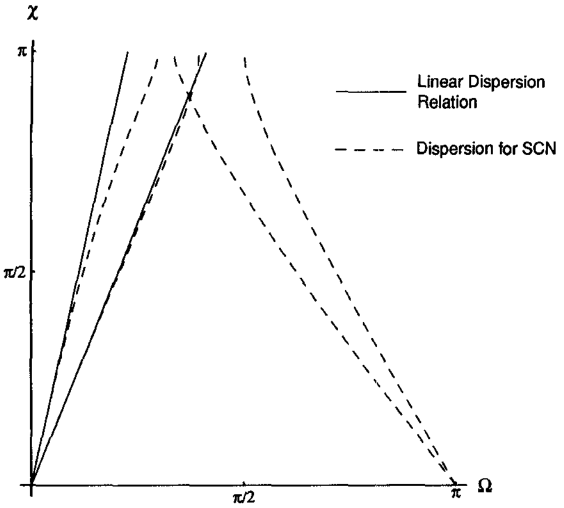

Fig. 1. Dispersion diagram for propagation in (1, 0, 0) direction, SCN with stubs, anisotropic medium.

of the characteristic (10) for $0 < \Omega < \pi$ and corresponding to the four propagating plane wave solutions of Maxwell's equations, respectively (degeneration of the eigenvalues). For the SCN with stubs, two branches of the dispersion curve are identical with the two branches of the linear dispersion curve for frequencies approaching zero. The corresponding four eigenvectors represent physical eigenvectors. The other two branches do not converge to the branches of the linear dispersion curve, thus the corresponding four eigenvectors represent unphysical eigenvectors.

Considering wave propagation in (1, 1, 0) direction, we have $\chi = \eta$ as well as $\xi = 0$. Evaluating (23) we obtain the six eigenvalues

$$\lambda_{1,2} = 1$$

and

$$\lambda_{3,\cdots,6} = -1. \tag{40}$$

Again, the corresponding eigenvectors describe electro- and magnetostatic solutions and unphysical solutions, respectively. The other twelve eigenvalues $\lambda_{7,\cdots,18}$ are given implicitly by

$$C_{0i}\lambda^6 + C_{1i}\lambda^5 + C_{2i}\lambda^4 + 2C_{3i}\lambda^3 + C_{2i}\lambda^2 + C_{1i}\lambda + C_{0i} = 0 \tag{41}$$

and with $\lambda = e^{j\Omega}$ by

$$C_{0i}\cos(3\Omega) + C_{1i}\cos(2\Omega) + C_{2i}\cos(\Omega) + C_{3i} = 0. \tag{42}$$

The coefficients are

$$\begin{aligned}
C_{01} &= (4+Y_x)(4+Y_y)(4+Z_z)\\
C_{11} &= 4(4Y_x + 4Y_y + 2Y_xY_y + 8Z_z + 3Y_xZ_z\\
&\quad + 3Y_yZ_z + Y_xY_yZ_z)\cos(\chi)\\
&\quad + 2(64 + 8Y_x + 8Y_y - 2Y_xZ_z - 2Y_yZ_z - Y_xY_yZ_z)\\
C_{21} &= -2(16 + 4Y_x + 4Y_y - 4Z_z - 2Y_xZ_z\\
&\quad - 2Y_yZ_z - Y_xY_yZ_z)\cos(2\chi)\\
&\quad - 8(16 + 4Z_z + 2Y_xZ_z + 2Y_yZ_z + Y_xY_yZ_z)\\
&\quad \cdot \cos(\chi) + 96 - 8Y_x - 8Y_y - 4Y_xY_y\\
&\quad + 8Z_z + 8Y_xZ_z + 8Y_yZ_z + 5Y_xY_yZ_z\\
C_{31} &= -2(16 + 4Y_x + 4Y_y + 4Z_z + 2Y_xZ_z\\
&\quad + 2Y_yZ_z + Y_xY_yZ_z)\cos(2\chi) - 4(32 + 4Y_x\\
&\quad + 4Y_y + 2Y_xY_y - Y_xZ_z - Y_yZ_z - Y_xY_yZ_z)\\
&\quad \cdot \cos(\chi) + 4(8 - 2Y_x - 2Y_y - 6Z_z - 2Y_xZ_z\\
&\quad - 2Y_yZ_z - Y_xY_yZ_z)
\end{aligned} \tag{43}$$

and

$$\begin{aligned}
C_{02} &= (4+Y_z)(4+Z_x)(4+Z_y)\\
C_{12} &= 4(4Z_x + 4Z_y + 2Z_xZ_y + 8Y_z + 3Y_zZ_x\\
&\quad + 3Y_zZ_y + Y_zZ_xZ_y)\cos(\chi)\\
&\quad + 2(64 + 8Z_x + 8Z_y - 2Y_zZ_x - 2Y_zZ_y - Y_zZ_xZ_y)\\
C_{22} &= -2(16 + 4Z_x + 4Z_y - 4Y_z - 2Y_zZ_x\\
&\quad - 2Y_zZ_y - Y_zZ_xZ_y)\cos(2\chi)\\
&\quad - 8(16 + 4Y_z + 2Y_zZ_x + 2Y_zZ_y + Y_zZ_xZ_y)\\
&\quad \cdot \cos(\chi) + 96 - 8Z_x - 8Z_y - 4Z_xZ_y + 8Y_z\\
&\quad + 8Y_zZ_x + 8Y_zZ_y + 5Y_zZ_xZ_y\\
C_{32} &= -2(16 + 4Z_x + 4Z_y + 4Y_z + 2Y_zZ_x\\
&\quad + 2Y_zZ_y + Y_zZ_xZ_y)\cos(2\chi) - 4(32 + 4Z_x\\
&\quad + 4Z_y + 2Z_xZ_y - Y_zZ_x - Y_zZ_y - Y_zZ_xZ_y)\\
&\quad \cdot \cos(\chi) + 4(8 - 2Z_x - 2Z_y - 6Y_z\\
&\quad - 2Y_zZ_x - 2Y_zZ_y - Y_zZ_xZ_y).
\end{aligned} \tag{44}$$

The approximation of (42) for frequencies and wave numbers approaching zero yields

$$\begin{aligned}
&\left[4(8 + Y_x + Y_y)k_x^2 - (4+Y_x) \cdot (4+Y_y)(4+Z_z)\frac{\Delta t^2}{\Delta l^2}\omega^2\right]\\
&\left[4(8 + Z_x + Z_y)k_x^2 - (4+Y_z) \cdot (4+Z_x)(4+Z_y)\frac{\Delta t^2}{\Delta l^2}\omega^2\right] = 0
\end{aligned} \tag{45}$$

and

$$\left[(\varepsilon_{rx} + \varepsilon_{ry})k_x^2 - 4\varepsilon_{rx}\varepsilon_{ry}\mu_{rz}\frac{\Delta t^2}{\Delta l^2}\omega^2\right] \cdot \left[(\mu_x + \mu_y)k_x^2 - 4\varepsilon_{rz}\mu_{rx}\mu_{ry}\frac{\Delta t^2}{\Delta l^2}\omega^2\right] = 0 \tag{46}$$

in terms of ε_{ri} and μ_{ri}. Again, using $c_0/c_m = 1/2$, we obtain a result which is identical with the dispersion relation of the propagating plane wave solutions of Maxwell's equations, (11). Similar results may be calculated for wave propagation along the diagonal in the x–z- and y–z-plane.

Fig. 2 depicts the results of the numerical evaluation of (42) for a symmetric anisotropic medium with $\varepsilon_{rx} = 8$, $\varepsilon_{ry} = 2$, $\varepsilon_{rz} = 1.5$ and $\mu_{rx} = 2$, $\mu_{ry} = 1$, $\mu_{rz} = 2.5$. As in Fig. 1, there are two branches of the dispersion curve for the SCN which are identical with the two branches of the linear dispersion curve for frequencies approaching zero thus corresponding to four physical eigenvectors. There are four branches which do not converge to the branches of the linear dispersion curve. With each of these branches, one unphysical eigenvector is

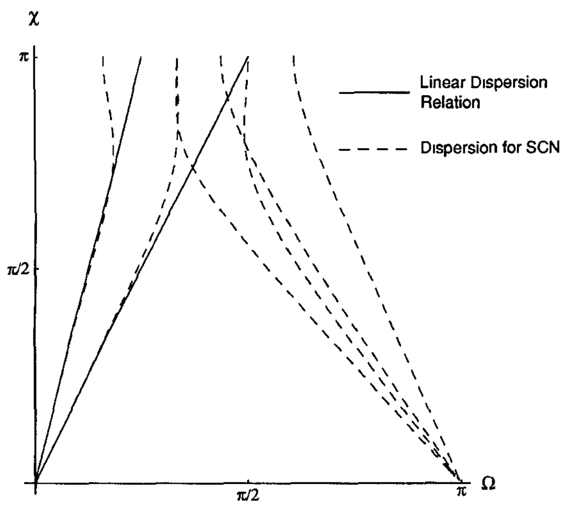

Fig. 2. Dispersion diagram for propagation in (1, 1, 0) direction, SCN with stubs, anisotropic medium.

associated so that there is no degeneration of the corresponding eigenvalues.

We investigate the wave propagation in isotropic media. For this case, we have $\varepsilon_{rx} = \varepsilon_{ry} = \varepsilon_{ry} = \varepsilon_r$ as well as $\mu_{rx} = \mu_{ry} = \mu_{rz} = \mu_r$ and therefore $Z_x = Z_y = Z_z = Z$ as well as $Y_x = Y_y = Y_z = Y$. In contrast to (12), the evaluation of (23) does not yield a simple algebraic expression. Thus, for isotropic media, we only consider wave propagation in (1, 0, 0) direction, in (1, 1, 0) direction and in (1, 1, 1) direction (along the space diagonal with respect to the TLM mesh). For wave propagation in (1, 0, 0) direction, the characteristic polynomials, (34), may not be simplified significantly assuming the isotropic case. For wave propagation in (1, 1, 0) direction, the polynomial in (41) splits in two parts. The eigenvalues $\lambda_{1,\cdots,6}$ are again given by (40), whereas the eigenvalues $\lambda_{7,\cdots,10}$ are given by

$$C_{0i}\lambda^2 + 2C_{1i}\lambda + C_{0i} = 0 \tag{47}$$

and with $\lambda = e^{j\Omega}$ by

$$C_{0i}\cos(\Omega) + C_{1i} = 0 \tag{48}$$

with

$$\begin{aligned} C_{01} &= 4 + Z, \\ C_{11} &= (2 + Z)\cos(\chi) + 2 \end{aligned} \tag{49}$$

and

$$\begin{aligned} C_{02} &= 4 + Y, \\ C_{12} &= (2 + Y)\cos(\chi) + 2. \end{aligned} \tag{50}$$

We approximate (48) for frequencies around $f = 1/(2\Delta t)$ using $\cos(x+\pi) \approx -1 + x^2/2$ and for wave numbers approaching zero using $\cos x \approx 1 - x^2/2$. We obtain

$$\left[(2+Z)k_x^2 - (4+Z)\frac{\Delta t^2}{\Delta l^2}\omega^2\right] \cdot \left[(2+Y)k_x^2 - (4+Y)\frac{\Delta t^2}{\Delta l^2}\omega^2\right] = 0 \tag{51}$$

and

$$\left[\left(1 - \frac{1}{2\mu_r}\right)k_x^2 - \frac{\Delta t^2}{\Delta l^2}\omega^2\right] \cdot \left[\left(1 - \frac{1}{2\varepsilon_r}\right)k_x^2 - \frac{\Delta t^2}{\Delta l^2}\omega^2\right] = 0 \tag{52}$$

respectively. The eigenvectors corresponding to these eigenvalues describe unphysical solutions propagating with a propagation velocity different from the propagation velocity of the physical solutions. However, using an excitation with a frequency spectrum bounded sufficiently below $f = 1/(2\Delta t)$, the unphysical solutions will not be excited and thus, they will not affect the accuracy of the field computation.

The other eight eigenvalues $\lambda_{11,\cdots,18}$are given by the following factors of the characteristic equation

$$C_{0i}\lambda^4 + C_{1i}\lambda^3 + 2C_{2i}\lambda^2 + C_{1i}\lambda + C_{0i} = 0 \tag{53}$$

and

$$C_{0i}\cos(2\Omega) + C_{1i}\cos(\Omega) + C_{2i} = 0 \tag{54}$$

respectively, specified by the two different sets of coefficients

$$\begin{aligned} C_{01} &= (4+Y)(4+Z) \\ C_{11} &= 2(2Y + YZ - 8)[\cos(\chi) - 1] \\ C_{21} &= YZ - 4Z - 2(8 + 2Y + YZ)\cos(\chi) \end{aligned} \tag{55}$$

and

$$\begin{aligned} C_{02} &= (4+Y)(4+Z) \\ C_{12} &= 2(2Z + YZ - 8)[\cos(\chi) - 1] \\ C_{22} &= YZ - 4Y - 2(8 + 2Z + YZ)\cos(\chi). \end{aligned} \tag{56}$$

As for wave propagation in (1, 0, 0) direction in isotropic media, for both sets of coefficients, (54) converges to the same linear dispersion relation for frequencies and wave numbers approaching zero. Using $\cos x \approx 1 - x^2/2$, we obtain

$$8k_x^2 - (Y+4)(Z+4)\frac{\Delta t^2}{\Delta l^2}\omega^2 = 0 \tag{57}$$

and

$$k_x^2 - 2\varepsilon_r\mu_r\frac{\Delta t^2}{\Delta l^2}\omega^2 = 0 \tag{58}$$

which is identical with (12) assuming $k_x = k_y$, $k_z = 0$, and $c_0/c_m = 1/2$.

For wave propagating in (1, 1, 1) direction and for $\chi = \eta = \xi$, respectively, there are again eighteen eigenvalues which are calculated from (23). The first two eigenvalues $\lambda_{1,2} = 1$ represent the electro- and magnetostatic case. Four eigenvalues $\lambda_{3,\cdots,6}$ are given implicitly by

$$C_{0i}\lambda^2 + 2C_{1i}\lambda + C_{0i} = 0 \tag{59}$$

thus we have with $\lambda = e^{j\Omega}$

$$C_{0i}\cos(\Omega) + C_{1i} = 0 \tag{60}$$

where either

$$\begin{aligned} C_{01} &= 4 + Z, \\ C_{11} &= 4 + Z\cos(\chi) \end{aligned} \tag{61}$$

or

$$C_{02} = 4 + Y,$$
$$C_{12} = 4 + Y\cos(\chi). \tag{62}$$

These eigenvalues represent unphysical solutions propagating with a propagation velocity different from the propagation velocity of the physical solutions. Approximating (60) for frequencies around $f = 1/(2\Delta t)$ using $\cos(x+\pi) \approx -1 + x^2/2$ and for wave numbers approaching zero using $\cos x \approx 1 - x^2/2$, we obtain

$$\left[Zk_x^2 - (4+Z)\frac{\Delta t^2}{\Delta l^2}\omega^2\right] \cdot \left[Yk_x^2 - (4+Y)\frac{\Delta t^2}{\Delta l^2}\omega^2\right] = 0 \tag{63}$$

and

$$\left[\left(1 - \frac{1}{\mu_r}\right)k_x^2 - \frac{\Delta t^2}{\Delta l^2}\omega^2\right] \cdot \left[\left(1 - \frac{1}{\varepsilon_r}\right)k_x^2 - \frac{\Delta t^2}{\Delta l^2}\omega^2\right] = 0. \tag{64}$$

The other twelve eigenvalues $\lambda_{7,\dots,18}$ are given by the polynomial

$$(C_0\lambda^6 + C_1\lambda^5 + C_2\lambda^4 + 2C_3\lambda^3 + C_2\lambda^2 + C_1\lambda + C_0)^2 = 0 \tag{65}$$

resulting in

$$[C_0\cos(3\Omega) + C_1\cos(2\Omega) + C_2\cos(\Omega) + C_3]^2 = 0 \tag{66}$$

with

$$\begin{aligned} C_0 &= (4+Y)(4+Z) \\ C_1 &= 2[2\cos(\chi)(2Y + 2Z + YZ) + 16 - YZ] \\ C_2 &= -2(12 - YZ)\cos(2\chi) - 8YZ\cos(\chi) \\ &\quad + 8 - 4Y - 4Z + 5YZ \\ C_3 &= -2(12 + YZ)\cos(2\chi) - 4(2Y + 2Z - YZ) \\ &\quad \cdot \cos(\chi) - 8 - 4YZ. \end{aligned} \tag{67}$$

Again, the approximation for frequencies and wave numbers approaching zero coincides with the linear dispersion relation of Maxwell's equations

$$12k_x^2 + (Y+4)(Z+4)\frac{\Delta t^2}{\Delta l^2}\omega^2 = 0 \tag{68}$$

and

$$3k_x^2 - 4\varepsilon_r\mu_r\frac{\Delta t^2}{\Delta l^2}\omega^2 = 0. \tag{69}$$

Approximating (66) for frequencies approaching zero using $\cos x \approx 1 - x^2/2$ and for wave numbers around $k_x = \pi/\Delta l$ using $\cos(x+\pi) \approx -1 + x^2/2$, we obtain

$$3k_x^2 - 4\frac{\Delta t^2}{\Delta l^2}\omega^2 = 0 \tag{70}$$

representing the dispersion relation of a unphysical solution propagating with the wave propagation velocity of the free space. This ambiguity of the dispersion relation for frequencies approaching zero leads to the appearance of spurious modes [11], [20], [21].

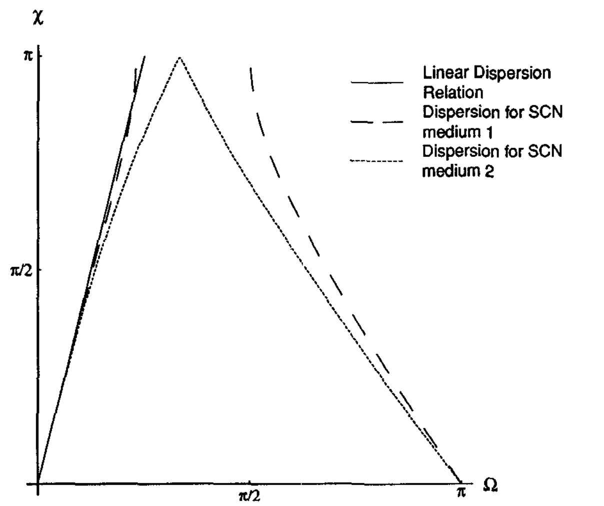

Fig. 3. Dispersion diagram for propagation in (1, 0, 0) direction, SCN with stubs, isotropic medium.

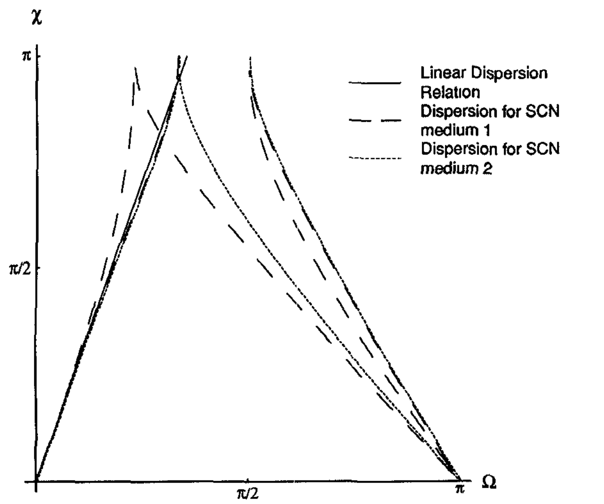

Fig. 4. Dispersion diagram for propagation in (1, 1, 0) direction, SCN with stubs, isotropic medium.

Figs. 3–5 illustrate the dispersion characteristics of the eigenvectors describing the propagating solutions of the TLM scheme for the stub-loaded SCN modeling an isotropic medium with $\varepsilon_r = 4$, $\mu_r = 1$ denoted by medium 1 and an isotropic medium with $\varepsilon_r = \mu_r = 2$ denoted by medium 2. Beside for frequencies approaching zero, the dispersion characteristics are different when modeling the two isotropic media. This is in contrast to the linear dispersion relation of Maxwell's equations. Note that for wave propagation in (1, 1, 0) direction, see Fig. 4, there are two branches of the dispersion curve for the SCN modeling medium 1 converging to the one branch of the linear dispersion curve. Each of these branches is associated with two physical eigenvectors. In all other cases, there is only one branch converging to the linear dispersion curve, thus these branches are associated with four physical eigenvectors.

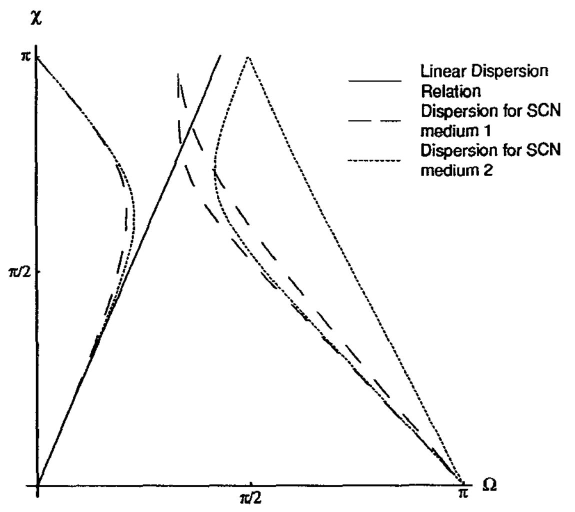

Fig. 5. Dispersion diagram for propagation in (1, 1, 1) direction, SCN with stubs, isotropic medium.

For the branches corresponding to physical eigenvectors, the deviations from the linear dispersion curve are both positive and negative depending on the value of the frequency. In [7], the existence of both positive and negative frequency errors was observed in dependence of the material parameters ε_r and μ_r and in dependence of the directions of wave propagation. Our results confirm this effect called bilateral dispersion. However, they also show that bilateral dispersion does not affect the accuracy of field computation if the discretization interval Δl is chosen sufficiently small. For wave propagation in (1, 1, 1) direction, the ambiguity of the dispersion relation for frequencies approaching zero becomes obvious. The different propagation velocities become apparent by the different gradients of the dispersion curves for frequencies approaching zero.

IV. The Dispersion Analysis of TLM with SSCN

The SSCN has been proposed recently by Trenkic *et al.* [5], [8]. The scattering at the SSCN is described by a symmetrical 12×12-matrix. We restrict our investigations to a regular mesh with $\Delta x = \Delta y = \Delta z = \Delta l$. In contrast to [5], [8], we normalize the wave amplitudes in terms of power amplitudes which is necessary to obtain a unitary scattering matrix given by

$$\boldsymbol{S} = \begin{bmatrix} \boldsymbol{\alpha}_1 & \boldsymbol{\beta}_1 & \boldsymbol{\beta}_2 \\ \boldsymbol{\beta}_1^T & \boldsymbol{\alpha}_2 & \boldsymbol{\beta}_3 \\ \boldsymbol{\beta}_2^T & \boldsymbol{\beta}_3^T & \boldsymbol{\alpha}_3 \end{bmatrix} \tag{71}$$

with (72), shown at the bottom of the next page, and

$$\boldsymbol{\beta}_1 = \begin{bmatrix} 0 & 0 & \frac{f}{1+f^2} & -\frac{f}{1+f^2} \\ 0 & 0 & -\frac{f}{1+f^2} & \frac{f}{1+f^2} \\ \frac{c}{1+c^2} & \frac{c}{1+c^2} & 0 & 0 \\ \frac{c}{1+c^2} & \frac{c}{1+c^2} & 0 & 0 \end{bmatrix}$$

$$\boldsymbol{\beta}_2 = \begin{bmatrix} 0 & 0 & \frac{b}{1+b^2} & \frac{b}{1+b^2} \\ 0 & 0 & \frac{b}{1+b^2} & \frac{b}{1+b^2} \\ \frac{e}{1+e^2} & -\frac{e}{1+e^2} & 0 & 0 \\ -\frac{e}{1+e^2} & \frac{e}{1+e^2} & 0 & 0 \end{bmatrix}$$

$$\boldsymbol{\beta}_3 = \begin{bmatrix} 0 & 0 & \frac{d}{1+d^2} & -\frac{d}{1+d^2} \\ 0 & 0 & -\frac{d}{1+d^2} & \frac{d}{1+d^2} \\ \frac{a}{1+a^2} & \frac{a}{1+a^2} & 0 & 0 \\ \frac{a}{1+a^2} & \frac{a}{1+a^2} & 0 & 0 \end{bmatrix} \tag{73}$$

wherein

$$\begin{aligned} a &= \sqrt{Z_{zx}/Z_{yx}} \\ b &= \sqrt{Z_{xy}/Z_{zy}} \\ c &= \sqrt{Z_{yz}/Z_{xz}} \\ d &= \sqrt{Z_{yz}/Z_{zy}} \\ e &= \sqrt{Z_{zx}/Z_{xz}} \\ f &= \sqrt{Z_{xy}/Z_{yx}}. \end{aligned} \tag{74}$$

The impedances $Z_{i,j}$ with $i, j \in \{x; y; z\}$ represent the normalized wave impedances of the transmission lines. The index i indicates the direction, the second index j the polarization of the line [5]. For $\Delta x = \Delta y = \Delta z = \Delta l$, the connection operator in wave vector domain is given by

$$\begin{aligned} \overline{\boldsymbol{\Gamma}} = {} & e^{-j\chi}(\boldsymbol{\Delta}_{1,2} + \boldsymbol{\Delta}_{3,4}) + e^{j\chi}(\boldsymbol{\Delta}_{2,1} + \boldsymbol{\Delta}_{4,3}) \\ & + e^{-j\eta}(\boldsymbol{\Delta}_{5,6} + \boldsymbol{\Delta}_{7,8}) + e^{j\eta}(\boldsymbol{\Delta}_{6,5} + \boldsymbol{\Delta}_{8,7}) \\ & + e^{-j\xi}(\boldsymbol{\Delta}_{9,10} + \boldsymbol{\Delta}_{11,12}) \\ & + e^{j\xi}(\boldsymbol{\Delta}_{10,9} + \boldsymbol{\Delta}_{12,11}). \end{aligned} \tag{75}$$

At first, we consider wave propagating in (1, 0, 0) direction in symmetric anisotropic media. The evaluation of (23) yields twelve eigenvalues. Four eigenvalues are given by

$$\lambda_{1,2} = 1$$

and

$$\lambda_{3,4} = -1 \tag{76}$$

representing again the electro- and magnetostatic case and unphysical solutions oscillating with the frequency $f = 1/(2\Delta t)$, respectively. The other eight eigenvalues $\lambda_{5,\cdots,12}$ are given implicitly by

$$C_{0i}\lambda^4 + C_{1i}\lambda^3 + 2C_{2i}\lambda^2 + C_{1i}\lambda + C_{0i} = 0 \tag{77}$$

and with $\lambda = e^{j\Omega}$ by

$$C_{0i}\cos(2\Omega) + C_{1i}\cos(\Omega) + C_{2i} = 0 \tag{78}$$

with the two sets of coefficients

$$\begin{aligned} C_{01} &= (1+c^2)(1+e^2) \\ C_{11} &= 2(e^2 - c^2)[\cos(\chi) - 1] \\ C_{21} &= (c^2 - 1)(1 - e^2) - 2(c^2 + e^2)\cos(\chi) \end{aligned} \tag{79}$$

and

$$\begin{aligned} C_{02} &= (1+b^2)(1+f^2) \\ C_{12} &= 2(b^2-f^2)[\cos(\chi)-1] \\ C_{22} &= (b^2-1)(1-f^2)-2(b^2+f^2)\cos(\chi). \end{aligned} \tag{80}$$

The approximating of (78) for frequencies and wave numbers approaching zero using $\cos x \approx 1 - x^2/2$ yields

$$\left[c^2k_x^2-(1+c^2)(1+e^2)\frac{\Delta t^2}{\Delta l^2}\omega^2\right] \cdot \left[f^2k_x^2-(1+b^2)(1+f^2)\frac{\Delta t^2}{\Delta l^2}\omega^2\right]=0. \tag{81}$$

Considering $c_0/c_m = 1/2$, the comparison of (81) to the linear dispersion relation of Maxwell's (10), requires

$$\begin{aligned} \varepsilon_{rz}\mu_{ry} &= \frac{(1+c^2)(1+e^2)}{4c^2} \\ \varepsilon_{ry}\mu_{rz} &= \frac{(1+b^2)(1+f^2)}{4f^2}. \end{aligned} \tag{82}$$

Evaluating the dispersion relation for wave propagation along the y- and z-axis in the same way, we obtain

$$\begin{aligned} \varepsilon_{rx}\mu_{rz} &= \frac{(1+a^2)(1+f^2)}{4a^2} \\ \varepsilon_{rz}\mu_{rx} &= \frac{(1+c^2)(1+d^2)}{4d^2} \\ \varepsilon_{rx}\mu_{ry} &= \frac{(1+a^2)(1+e^2)}{4e^2} \\ \varepsilon_{ry}\mu_{rx} &= \frac{(1+b^2)(1+d^2)}{4b^2}. \end{aligned} \tag{83}$$

These six relations yield the relations between the normalized impedances and ε_{ri}, μ_{ri}

$$\begin{aligned} \varepsilon_{rx} &= \frac{1}{2}\left(\frac{1}{Z_{yx}}+\frac{1}{Z_{zx}}\right) \\ \varepsilon_{ry} &= \frac{1}{2}\left(\frac{1}{Z_{xy}}+\frac{1}{Z_{zy}}\right) \\ \varepsilon_{rz} &= \frac{1}{2}\left(\frac{1}{Z_{xz}}+\frac{1}{Z_{yz}}\right) \\ \mu_{rx} &= \frac{Z_{yz}+Z_{zy}}{2} \\ \mu_{ry} &= \frac{Z_{xz}+Z_{zx}}{2} \\ \mu_{rz} &= \frac{Z_{xy}+Z_{yx}}{2}. \end{aligned} \tag{84}$$

Equations (82) and (83) represent the basis for a correct modeling of symmetric anisotropic media using the SSCN. Note that exchanging ε_{ri} and μ_{ri} in these equations yields the same set of eigenvalues in the dispersion analysis of the SSCN. However, the corresponding eigenvectors do not converge to the eigenvectors of Maxwell's equations for frequencies approaching zero.

The dispersion in a TLM mesh for wave propagation in (1, 0, 0) direction in a symmetric anisotropic medium with $\varepsilon_{rx} = 8$, $\varepsilon_{ry} = 2$, $\varepsilon_{rz} = 1.5$ and $\mu_{rx} = 2$, $\mu_{ry} = 1$, $\mu_{rz} = 2.5$ is illustrated in Fig. 6. Calculating the parameters of the scattering matrix from (82) and (83), we obtain two sets of parameters resulting in two different dispersion relations. For one set, the parameters a, b, c, d, e, and f have low values (the dispersion curves are denoted by Z1), for the other set,

$$\boldsymbol{\alpha}_1 = \begin{bmatrix} \frac{1-b^2f^2}{(1+b^2)(1+f^2)} & \frac{-b^2+f^2}{(1+b^2)(1+f^2)} & 0 & 0 \\ \frac{-b^2+f^2}{(1+b^2)(1+f^2)} & \frac{1-b^2f^2}{(1+b^2)(1+f^2)} & 0 & 0 \\ 0 & 0 & \frac{-1+c^2e^2}{(1+c^2)(1+e^2)} & \frac{c^2-e^2}{(1+c^2)(1+e^2)} \\ 0 & 0 & \frac{c^2-e^2}{(1+c^2)(1+e^2)} & \frac{-1+c^2e^2}{(1+c^2)(1+e^2)} \end{bmatrix}$$

$$\boldsymbol{\alpha}_2 = \begin{bmatrix} \frac{1-c^2d^2}{(1+c^2)(1+d^2)} & \frac{-c^2+d^2}{(1+c^2)(1+d^2)} & 0 & 0 \\ \frac{-c^2+d^2}{(1+c^2)(1+d^2)} & \frac{1-c^2d^2}{(1+c^2)(1+d^2)} & 0 & 0 \\ 0 & 0 & \frac{-1+a^2f^2}{(1+a^2)(1+f^2)} & \frac{a^2-f^2}{(1+a^2)(1+f^2)} \\ 0 & 0 & \frac{a^2-f^2}{(1+a^2)(1+f^2)} & \frac{-1+a^2f^2}{(1+a^2)(1+f^2)} \end{bmatrix}$$

$$\boldsymbol{\alpha}_3 = \begin{bmatrix} \frac{1-a^2e^2}{(1+a^2)(1+e^2)} & \frac{-a^2+e^2}{(1+a^2)(1+e^2)} & 0 & 0 \\ \frac{-a^2+e^2}{(1+a^2)(1+e^2)} & \frac{1-a^2e^2}{(1+a^2)(1+e^2)} & 0 & 0 \\ 0 & 0 & \frac{-1+b^2d^2}{(1+b^2)(1+d^2)} & \frac{b^2-d^2}{(1+b^2)(1+d^2)} \\ 0 & 0 & \frac{b^2-d^2}{(1+b^2)(1+d^2)} & \frac{-1+b^2d^2}{(1+b^2)(1+d^2)} \end{bmatrix} \tag{72}$$

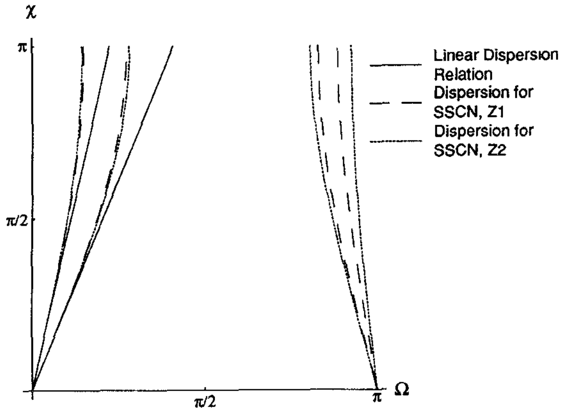

Fig. 6. Dispersion diagram for propagation in (1, 0, 0) direction, SSCN, anisotropic medium.

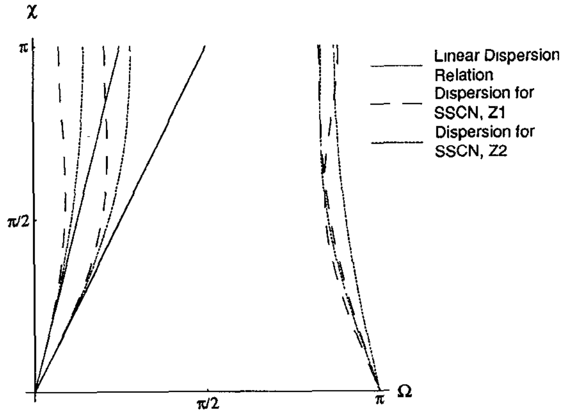

Fig. 7. Dispersion diagram for propagation in (1, 1, 0) direction, SSCN, anisotropic medium.

the values of the parameters are high (the dispersion curves are denoted by Z2). As for the SCN with stubs, two branches of the dispersion curve are identical with the two branches of the linear dispersion curve for frequencies approaching zero (four physical eigenvectors), whereas the other two branches do not converge to the branches of the linear dispersion curve (four unphysical eigenvectors).

Considering wave propagation in (1, 1, 0) direction, we obtain the same four eigenvalues as in (76). The other eight eigenvalues $\lambda_{5,\ldots,12}$ are given implicitly by

$$C_{0i}\lambda^4 + C_{1i}\lambda^3 + 2C_{2i}\lambda^2 + C_{1i}\lambda + C_{0i} = 0 \qquad (85)$$

resulting in

$$C_{0i}\cos(2\Omega) + C_{1i}\cos(\Omega) + C_{2i} = 0 \qquad (86)$$

with

$$\begin{aligned} C_{01} &= (1+c^2)(1+d^2)(1+e^2) \\ C_{11} &= 2(1+c^2)(e^2-d^2)[\cos(\chi)-1] \\ C_{21} &= (d^2+e^2)(1+c^2) - 1 - c^2d^2e^2 \\ &\quad - 2(1+c^2)(d^2+e^2)\cos(\chi) \\ &\quad - (c^2+d^2e^2)\cos(2\chi) \end{aligned} \qquad (87)$$

and

$$\begin{aligned} C_{02} &= (1+a^2)(1+b^2)(1+f^2) \\ C_{12} &= 2(b^2-a^2)(1+f^2)[\cos(\chi)-1] \\ C_{22} &= (a^2+b^2)(1+f^2) - 1 - a^2b^2f^2 \\ &\quad - 2(1+f^2)(a^2+b^2)\cos(\chi) \\ &\quad - (f^2+a^2b^2)\cos(2\chi). \end{aligned} \qquad (88)$$

The approximation of (86) for frequencies and wave numbers approaching zero yields

$$\left[(c^2+d^2+c^2d^2+d^2e^2)k_x^2 - (1+c^2)(1+d^2)(1+e^2)\frac{\Delta t^2}{\Delta l^2}\omega^2\right] \left[(a^2+f^2+a^2b^2+a^2f^2)k_x^2 - (1+a^2)(1+b^2)(1+f^2)\frac{\Delta t^2}{\Delta l^2}\omega^2\right] = 0 \qquad (89)$$

and in terms of ε_{ri} and μ_{ri}

$$\left[(\mu_{rx}+\mu_{ry})k_x^2 - 4\varepsilon_{rz}\mu_{rx}\mu_{ry}\frac{\Delta t^2}{\Delta l^2}\omega^2\right] \cdot \left[(\varepsilon_{rx}+\varepsilon_{ry})k_x^2 - 4\varepsilon_{rx}\varepsilon_{ry}\mu_{rz}\frac{\Delta t^2}{\Delta l^2}\omega^2\right] = 0 \qquad (90)$$

confirming (84), as the approximation is identical with the dispersion relation of Maxwell's equations, (11).

Fig. 7 depicts the results of the numerical evaluation of (86) for a symmetric anisotropic medium with $\varepsilon_{rx} = 8$, $\varepsilon_{ry} = 2$, $\varepsilon_{rz} = 1.5$ and $\mu_{rx} = 2$, $\mu_{ry} = 1$, $\mu_{rz} = 2.5$. Again, the dispersion curves for the set of the parameters a, b, c, d, e, and f with low values are denoted by Z1, whereas the dispersion curves for the set of parameters with high values are denoted by Z2. In contrast to the stub-loaded SCN, there are only two branches which do not converge to the branches of the linear dispersion curve (degeneration of the eigenvalues).

Considering isotropic media, we insert the conditions $\varepsilon_{rx} = \varepsilon_{ry} = \varepsilon_{rz} = \varepsilon_r$ and $\mu_{rx} = \mu_{ry} = \mu_{rz} = \mu_r$ in (84) and obtain two sets of the normalized impedances

$$\begin{aligned} Z_{xy} &= \sqrt{\frac{\mu_r}{\varepsilon_r}}(\alpha \pm \beta) \\ Z_{yz} &= \sqrt{\frac{\mu_r}{\varepsilon_r}}(\alpha \pm \beta) \\ Z_{zx} &= \sqrt{\frac{\mu_r}{\varepsilon_r}}(\alpha \pm \beta) \\ Z_{xz} &= \sqrt{\frac{\mu_r}{\varepsilon_r}}(\alpha \mp \beta) \\ Z_{yx} &= \sqrt{\frac{\mu_r}{\varepsilon_r}}(\alpha \mp \beta) \\ Z_{zy} &= \sqrt{\frac{\mu_r}{\varepsilon_r}}(\alpha \mp \beta) \end{aligned} \qquad (91)$$

where we have introduced

$$\alpha = \sqrt{\varepsilon_r\mu_r}$$

and

$$\beta = \sqrt{\varepsilon_r\mu_r - 1}. \qquad (92)$$

Equation (91) has already been derived considering the network model of the SSCN [22]. For isotropic media, both sets

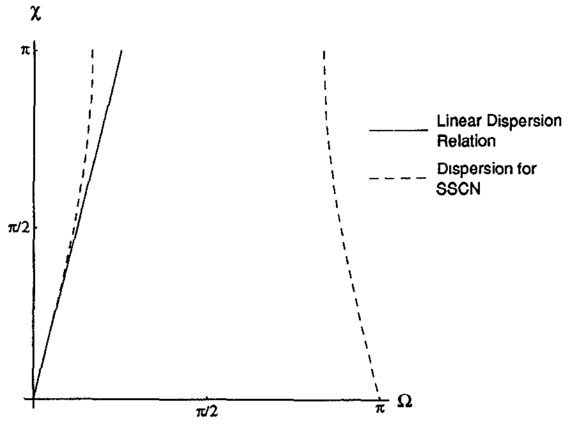

Fig. 8. Dispersion diagram for propagation in (1, 0, 0) direction, SSCN, isotropic medium.

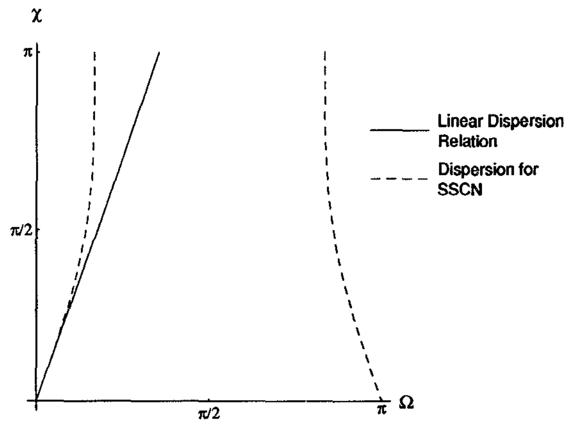

Fig. 9. Dispersion diagram for propagation in (1, 1, 0) direction, SSCN, isotropic medium.

of the impedances result in the same dispersion characteristics and in the same wave propagation velocities, respectively. The two sets of impedances lead to the same results for the field computation, if the difference of the impedances is taken into account in the mapping between the wave amplitudes and the field components [23].

Evaluating (23) for isotropic media, we obtain the same four eigenvalues as in (76). The other eight eigenvalues $\lambda_{5,\cdots,12}$ are given by the polynomial

$$(C_0\lambda^4 + C_1\lambda^2 + C_0)^2 = 0 \tag{93}$$

with

$$\begin{aligned} C_0 &= -\varepsilon_r\mu_r \\ C_1 &= 2\varepsilon_r\mu_r - 3 + \cos(\chi)\cos(\eta) + \cos(\chi) \\ &\quad \cdot \cos(\xi) + \cos(\eta)\cos(\xi) \end{aligned} \tag{94}$$

resulting in

$$\begin{aligned} 4\varepsilon_r\mu_r \sin^2(\Omega) &= 3 - \cos(\chi)\cos(\eta) - \cos(\chi) \\ &\quad \cdot \cos(\xi) - \cos(\eta)\cos(\xi) \end{aligned} \tag{95}$$

which is identical with the result given in [8]. The approximation of (95) for frequencies and wave numbers approaching zero and the approximation of (95) for frequencies around $f = 1/(2\Delta t)$ and for wave numbers approaching zero yield the same result,

$$\begin{aligned} k_x^2 + k_y^2 + k_z^2 &= 4\varepsilon_r\mu_r \frac{\Delta t^2}{\Delta l^2}\omega^2 \\ &= 0. \end{aligned} \tag{96}$$

As for the SCN with stubs, the ambiguity of the dispersion relation for frequencies approaching zero leads to the appearance of spurious modes [11], [20], [21].

Figs. 8, 9, and 10 illustrate the dispersion characteristics of the eigenvectors describing the propagating solutions of the TLM scheme for the SSCN modeling an isotropic medium with $\varepsilon_r\mu_r = 4$. In contrast to the SCN with stubs, the dispersion characteristics in a TLM mesh with SSCN's are only dependent on the product of ε_r and μ_r corresponding to the linear dispersion characteristics for isotropic media, (12).

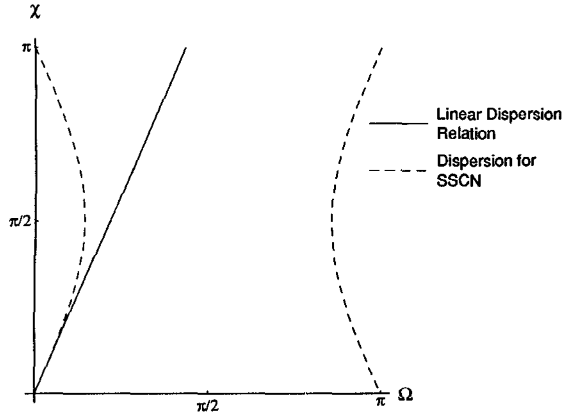

Fig. 10. Dispersion diagram for propagation in (1, 1, 1) direction, SSCN, isotropic medium.

V. Conclusion

A systematic dispersion analysis and a detailed discussion of unphysical solutions has been given for the SCN with stubs and for the SSCN. It has been shown that the modeling of symmetric anisotropic media using the SCN with stubs leads to correct results and to results converging to solutions of Maxwell's equations for frequencies and wave numbers approaching zero, respectively. However, there are nonphysical eigenvectors describing solutions of the TLM scheme which do not converge to solutions of Maxwell's equations. These unphysical solutions describe modes approaching a frequency $f = 1/(2\Delta t)$ for wave numbers approaching zero. For the SCN with stubs, there are unphysical eigenvectors describing nonpropagating solutions of the TLM scheme. Furthermore, there are unphysical eigenvectors describing propagating solutions of the TLM scheme with a propagation velocity different from the propagation velocity of the physical solutions.

For the SSCN, there are six relations between the relative permittivity and relative permeability and the parameters of the scattering matrix. These six relations provide the basis for a correct modeling of symmetric anisotropic media using the SSCN. The mapping of the parameters of the scattering matrix on the parameters describing the symmetric anisotropic medium is not bijective. For given material parameters, there exist two different solutions for the scattering matrix and the transmission line impedances yielding two different dispersion characteristics. However, both solutions result in the correct modeling of the electromagnetic field for frequencies approaching zero, if the difference in the transmission line impedances is considered in the mapping between the wave amplitudes and the field components [23]. Also for the SSCN, there are unphysical eigenvectors. In contrast to the stub-loaded SCN, these eigenvectors describe solutions propagating with the same propagation velocities as the propagation velocities of the physical solutions.

The dispersion characteristics of the SSCN are superior to the dispersion characteristics of the stub-loaded SCN. However, for both nodes, there is an ambiguity of the dispersion relation for frequencies approaching zero leading to the appearance of spurious modes. Thus both nodes exhibit disadvantages with respect to the dispersion characteristics when comparing them to the expanded and the asymmetrical condensed TLM node or with the FDTD method [13].

REFERENCES

[1] K. S. Yee, "Numerical solution of initial boundary value problems involving Maxwell's equations in isotropic media," *IEEE Trans. Antennas Propagat.*, vol. AP-14, no. 3, pp. 302–307, May 1966.

[2] W. J. R. Hoefer, "The transmission line matrix (TLM) method," in *Numerical Techniques for Microwave and Millimeter Wave Passive Structures*, T. Itoh, Ed. New York: Wiley, 1989, ch. 8, pp. 496–591.

[3] P. B. Johns, "A symmetrical condensed node for the TLM-method," *IEEE Trans. Microwave Theory Tech.*, vol. MTT-35, no. 4, pp. 370–377, Apr. 1987.

[4] R. Scaramuzza and A. J. Lowery, "Hybrid symmetrical condensed node for the TLM method," *Electron. Lett.*, vol. 26, no. 23, pp. 1947–1949, 1990.

[5] V. Trenkic, C. Christopoulos, and T. M. Benson, "Generally graded TLM mesh using the symmetrical supercondensed node," *Electron. Lett.*, vol. 30, no. 10, pp. 795–797, May 1994.

[6] M. Celuch-Marcysiak and W. K. Gwarek, "Toward better understanding of the SCN TLM method for inhomogeneous problems," in *Second Int. Workshop on Discrete Time Domain Modeling of Electromagnetic Fields and Networks*, German IEEE MTT/AP joint chapter and CAS chapter, Berlin, Oct. 1993.

[7] ——, "On the effect of bilateral dispersion in inhomogeneous symmetrical condensed node modeling," *IEEE Trans. Microwave Theory Tech.*, vol. 42, no. 6, pp. 1069–1073, June 1994.

[8] V. Trenkic, C. Christopoulos, and T. M. Benson, "Dispersion analysis of the TLM symmetrical super-condensed node," *Electron. Lett.*, vol. 30, no. 25, pp. 2151–2153, Dec. 1994.

[9] L. N. Trefethen "Group velocity in finite difference schemes," *SIAM Rev.*, vol. 24, no. 2, Apr. 1982.

[10] D. R. Lynch and K. D. Paulsen, "Origin of vector parasites in numerical Maxwell solution," *IEEE Trans. Microwave Theory Tech.*, vol. 39, no. 3, pp. 383–394, Mar. 1991.

[11] M. Krumpholz and P. Russer, "On the dispersion in TLM and FDTD," *IEEE Trans. on Microwave Theory and Tech.*, vol. 42, no. 7, pp. 1275–1279, July 1994.

[12] ——, "A generalized method for the calculation of TLM dispersion relations," in *Proc. 23th EMC*, Madrid, Sept. 1993, pp. 288–291.

[13] ——, "A field theoretical comparison of FDTD and TLM," to be published in the *IEEE Trans. Microwave Theory Tech.*

[14] P. Russer and M. Krumpholz, "The Hilbert space formulation of the TLM method," *Int. J. Numerical Modeling: Electronic Networks, Devices and Fields*, vol. 6, no. 1, pp. 29–45, Feb. 1993.

[15] M. Krumpholz and P. Russer, "Two-dimensional FDTD and TLM," *Int. J. Numerical Modeling: Electronic Networks, Devices and Fields*, vol. 7, pp. 141–153, Mar.–Apr. 1994.

[16] ——, "A field theoretical derivation of TLM," *IEEE Trans. Microwave Theory Tech.*, vol. 42, no. 9, pp. 1660–1668, Sept. 1994.

[17] W. Schroeder and I. Wolff, "The origin of spurious modes in numerical solutions of electromagnetic field eigenvalue problems," *IEEE Trans. Microwave Theory Tech.*, vol. 42, no. 4, pp. 644–653, Apr. 1994.

[18] J. L. Davis, *Wave Propagation in Electromagnetic Media.* New York: Springer-Ve.lag, 1990, pp. 99–127.

[19] P. Russer and M. Krumpholz, "On the field theoretical foundation of the transmission line matrix method," in *Second Int. Workshop Discrete Time Domain Modeling of Electromagnetic Fields and Networks*, German IEEE MTT/AP joint chapter and CAS chapter, Berlin, Oct. 1993.

[20] J. S. Nielsen, "TLM analysis of microwave and millimeter wave structures with embedded nonlinear devices," Ph.D. dissertation, Univ. of Ottawa, 1992.

[21] J. S. Nielsen and W. J. R. Hoefer, "A complete dispersion analysis of the condensed node TLM mesh," *IEEE Trans. Magn.*, vol. 27, no. 5, pp. 3982–3985, Sept. 1991.

[22] V. Trenkic, C. Christopoulos, and T. M. Benson, "A graded symmetrical super-condensed node for the TLM method," in *IEEE AP-S Int. Symp. 1994*, Seattle, WA, June 1994.

[23] M. Krumpholz, P. Russer, Q. Zhang, and W. J. R. Hoefer, "Field-theoretic foundation of two-dimensional TLM based on a rectangular mesh," in *IEEE MTT-S Int. Microwave Symp. Dig.*, San Diego, May 1994, pp. 333–336.

Christian Huber was born in Wasserburg/Inn, Germany, in 1966. He received the Dipl.-Ing. degree in electrical engineering from the Technical University Munich in 1991.

Since 1993 he has worked at the Ferdinand-Braun-Institut für Höchstfrequenztechnik in Berlin.

Michael Krumpholz (M'95) was born in Bonn, Germany, in 1966. He received the Dipl.-Ing. degree and the Dr.-Ing. degree in electrical engineering at the Technische Universität München in 1991 and 1994, respectively.

From 1991 to 1992, he worked as a Research Assistant at the Lehrstuhl für Hochfrequenztechnik, Technische Universität München. In 1992, he joined the Ferdinand-Braun-Institut für Höchstfrequenztechnik Berlin. Since 1994, he has worked as a Research Scientist at the Radiation Laboratory of the University of Michigan in Ann Arbor. His current research interests are numerical methods for the solution of Maxwell's equations.

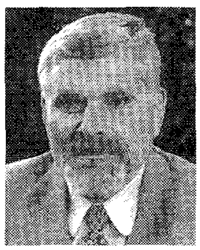

Peter Russer (SM'81–F'94) was born in Vienna, Austria, in 1943. He received the Dipl.-Ing. degree in 1967 and the Dr.Techn. degree in 1971, both in electrical engineering and both from the Technische Universität in Vienna, Austria.

From 1968 to 1971, he was an Assistant Professor at the Technische Universität in Vienna. In 1971, he joined the Research Institute of AEG-Telefunken in Ulm, where he worked on fiber-optic communication, broadband and low-noise solid-state electronic circuits, statistical noise analysis of microwave circuits, laser modulation, and fiber-optic gyroscopes. Since 1981 he has held the chair of Hochfrequenztechnik at the Technische Universität München. Since Oct. 1992, he has been Director of the Ferdinand-Braun-Institut für Höchstfrequenztechnik in Berlin. His current research interests are integrated microwave and millimeterwave circuits, electromagnetic fields, and methods for computer-aided design of microwave circuits. He is author of numerous scientific papers in these areas.

Dr. Russer is IEEE Fellow and member of the German Informationstechnische Gesellschaft and the Austrian and German Physical Societies. In 1979, he was corecipient of the NTG award.